Evidence for magnon excitation contribution to the magnetoresistance behavior during thermal annealing in CoFeB/MgO/CoFeB magnetic tunnel junctions

Q. L. Ma,[1] S. G. Wang,[1,*] H. X. Wei,[1] H. F. Liu,[1] X.-G. Zhang,[2] and X. F. Han[1]

[1]*State Key Laboratory of Magnetism, Beijing National Laboratory for Condensed Matter Physics, Institute of Physics,*
Chinese Academy of Sciences, Beijing 100190, China

[2]*Center for Nanophase Materials Sciences and Computer Science and Mathematics Division, Oak Ridge National Laboratory,*
P. O. Box 2008, Oak Ridge, Tennessee 37831-6493, USA

For sputtered CoFeB/MgO/CoFeB magnetic tunnel junctions, it is well known that the tunnel magnetoresistance (TMR) ratio increases with increasing annealing temperature (T_a) up to a critical value (T_p), and then decreases with further increasing T_a, resulting in a peak around T_p. The improved crystallinity of the MgO barrier and CoFeB electrodes due to annealing has been considered as the main reason for the enhancement of the TMR ratio, especially for $T_a < T_p$. In this work, the evidence is provided that the magnon excitation plays a great contribution to the magnetoresistance (MR) behavior in annealed samples based on the measurement of dynamic conductance and inelastic electron tunneling (IET) spectra. The magnon activation energy (E_c) obtained from the fits for IET spectra exhibits a similar temperature dependence with that of the TMR ratio. A detailed analysis shows that the magnon excitation, together with improved crystallinity of the MgO barrier and CoFeB layers, is the main contribution to the annealing-temperature-dependent MR behavior.

PACS number(s): 85.75.−d, 75.70.Cn, 75.30.Hx

MgO-based magnetic tunnel junctions (MTJs) have been investigated widely due to their interesting fundamental physics and potential applications.[1–8] Thermal annealing is a critical process for sputtered CoFeB/MgO/CoFeB junctions because the tunnel magnetoresistance (TMR) ratio of junctions annealed at an appropriate temperature increases dramatically.[9–13] Annealing greatly improves the crystallinity of the MgO barrier and ferromagnetic (FM) CoFeB electrodes as well as the interfaces between the MgO and CoFeB layers,[10,12] which enhances spin-dependent tunneling across the MgO barrier. The effects of thermal annealing were studied using transmission electron microscopy (TEM), x-ray photoelectron spectroscopy (XPS), and x-ray diffraction (XRD),[10,12,14–16] with a focus on the structural characterization.

For MTJs, the measurement of dynamic conductance (dI/dV) and the inelastic electron tunnel (IET) spectrum (d^2I/dV^2) has been proven to be a powerful tool to study spin-dependent tunneling.[16–24] Using this method, the influence of the density of states (DOS) and the inelastic scattering process on conductance can be clarified by measuring the first and second derivative of conductance.[24,25] Here, we report a detailed investigation of the dynamic conductance and IET spectra in CoFeB/MgO/CoFeB junctions as a function of annealing temperature T_a, with a focus on the magnetoresistance (MR) behavior. Our results show that magnon excitation contributes greatly to the annealing-temperature-dependent MR behavior.

Multilayers with a core structure of NiFe(5)/IrMn(10)/ CoFe(2)/Ru(0.8)/CoFeB(3)/MgO(2.5)/CoFeB(3) (in nm) were grown in a Shamrock sputtering system, where NiFe, IrMn, CoFe, and CoFeB stand for $Ni_{81}Fe_{19}$, $Ir_{22}Mn_{78}$, $Co_{90}Fe_{10}$, and $Co_{40}Fe_{40}B_{20}$, respectively. The bottom synthetic NiFe/IrMn/CoFe/Ru structure is used to pin the CoFeB layer via exchange bias. Thermal annealing was carried out in a vacuum system with a base pressure of 3×10^{-5} Pa in a magnetic field of 400 Oe. Dynamic conductance and IET spectra were measured at 5 K at 30.79 Hz with an ac modulation voltage of 4 mV using a standard lock-in method. XPS measurements were carried out on a Thermo Scientific ESCALAB 250 machine. The details of sample growth, junction fabrication, and measurement setup can be found elsewhere.[13,24–27]

Figure 1 shows the MR ratio [$(R_{AP}/R_P - 1) \times 100\%$] measured at room temperature (RT) as a function of annealing temperature T_a, similar to the results reported before,[11,12] where $R_{AP,P}$ stand for the resistance in the antiparallel (AP) and parallel (P) configurations, respectively. The MR ratio increases gradually as T_a is first increased, and then it dramatically increases when $T_a > 300\,°C$. It reaches a maximum at 375 °C, and then decreases with further increasing T_a, resulting in a peak (the peak temperature is called T_p). The dramatic increase of the MR ratio (larger than 100%) as $T_a > 300\,°C$ indicates a great improvement in crystallinity of the MgO barrier and the formation of single-crystalline CoFeB layers due to annealing.[1,10,12] Here, the focus is on four typical samples: junction A (as-grown sample), junction B with $T_a = 300\,°C$, junction C with $T_a = 375\,°C$, and junction D with $T_a = 400\,°C$, where junctions B, C, and D are underannealed, well annealed, and overannealed, respectively. The annealing-temperature dependence of the MR ratio shown above has been considered as a characteristic of sputtered CoFeB/MgO/CoFeB junctions. The increasing part of the MR ratio as a function of T_a has been mainly attributed to the improved crystallinity of the MgO barrier and the CoFeB layers during the annealing process. The decreasing part for $T_a > T_p$ is still an open issue, which will be discussed in detail.

The dynamic conductance as a function of bias voltage in the parallel and antiparallel configurations is shown in Fig. 2. For junction A, shown in Figs. 2(a) and 2(b), dI/dV-V curves do not show any features, similar to that in AlO_x-based MTJs,[28] indicating no coherent tunneling through the MgO barrier.
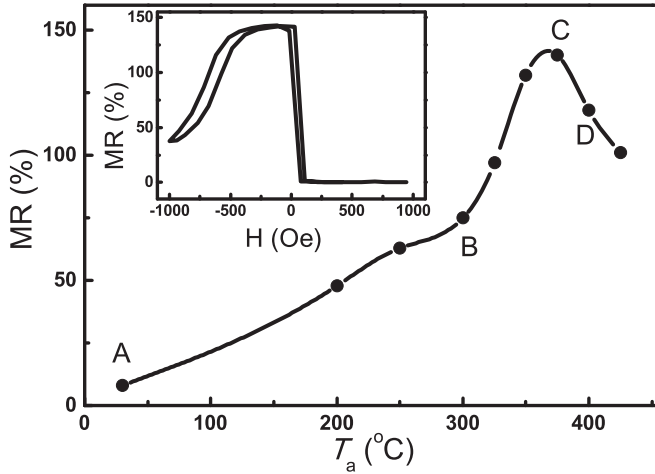
FIG. 1. TMR ratio as a function of annealing temperature (T_a). Inset: *R-H* loop at RT with $T_a = 375\,°C$.

For thermally annealed samples, dI/dV-V curves in the P state [shown in Figs. 2(c), 2(e), and 2(g)] show some peaks, a characteristic of spin-dependent tunneling through the MgO barrier.[16,24] A clear asymmetry between positive and negative biases is also observed, due to different electronic structures of the top and bottom CoFeB/MgO interfaces,[10,12] although the structure is stoichiometrically symmetric. An even stronger asymmetry has been observed already in epitaxial Fe/MgO/Fe junctions[4,5,24] with a stoichiometrically symmetric structure as well, which was attributed to the fine interfacial structure including vacancies and the formation of an ultrathin FeO layer at the interfaces. For dI/dV-V curves in the AP state shown on the right-hand side of Fig. 2, there is an obvious shoulder at ∼200 mV for annealed junctions, originating from the band structure of CoFeB electrodes.[18,20] Therefore, thermal annealing plays a crucial role in spin-dependent tunneling, evidenced by the MR ratio and the dynamic conductance measurement.
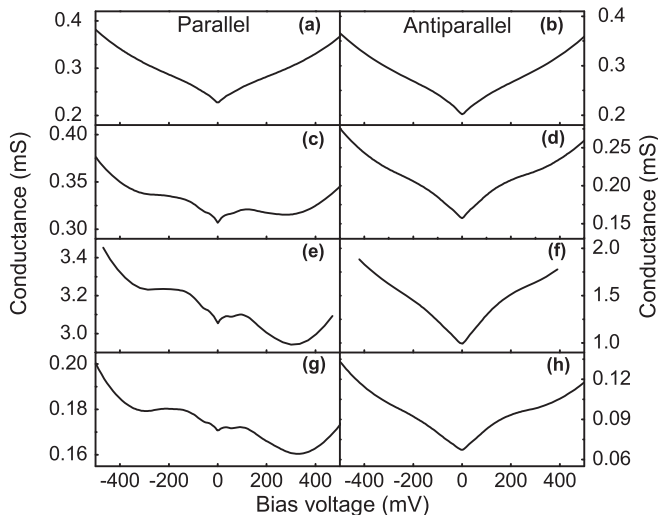

FIG. 2. Dynamic conductance for junction A (a), (b), B (c), (d), C (e), (f), and D (g), (h), respectively.
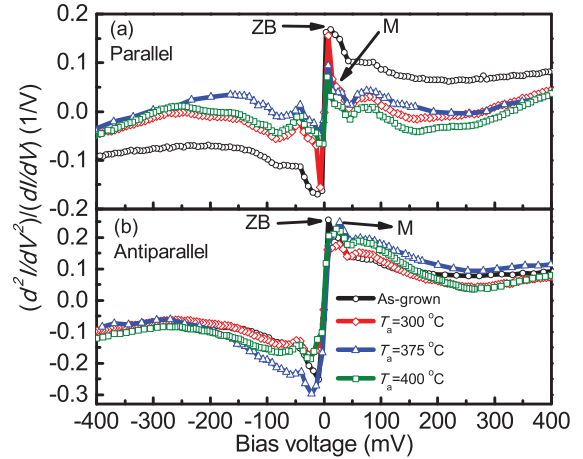

FIG. 3. (Color online) IET spectra for junctions A, B, C, and D for the P (a) and AP (b) configurations, respectively.

Figure 3 shows the normalized IET spectra for the P and AP states, where several peaks can be identified in the spectra. The zero-bias anomaly (marked by ZB) is clearly visible in both P and AP states, which comes from magnetic impurity scattering.[22,28,29] The ZB anomaly peak is independent of the configuration of the two FM electrodes. Our focus will be given to the peak located at ∼25 mV (marked by M). This peak is hardly visible for the as-grown sample shown by black open circles in Fig. 3(a). Furthermore, its intensity is much larger in the AP state than in the P state for annealed samples. This peak has been well known and is attributed to the magnon excitation.[21–23] The IET spectrum contains information from inelastic excitations including magnon, magnetic impurity scattering, and phonon and the background conductance. The background conductance and phonon excitation show a spin-independent behavior. For example, the magnetic state can be changed (from the P state to the AP state and vice versa) by an externally applied magnetic field, but the peaks due to the spin-independent process will not be affected. Therefore, the difference in the IET spectra between the P and AP states originates from the spin-dependent process.[17] Our main aim is the discussion of annealing effect on spin-dependent tunneling and the characteristic behavior of the MR ratio shown in Fig. 1.

Very recently, an analytic expression for contributions to the IET spectrum from surface magnon scattering and magnetic impurity scattering[25] has been carried out. It shows that surface magnon scattering alone does not lead to any peaks in the IET spectra, and only produces an IET spectrum consisting of three flat plateaus with discontinuities at $eV = \pm E_c$, where e, V, E_c stand for the electron mass, bias voltage, and magnon activation energy, respectively. The peaks at low bias voltage observed in the IET spectra are due to magnetic impurity scattering, in good agreement with the traditional model for the zero-bias anomaly. Magnetic impurity scattering produces a logarithm singularity in the conductance, which corresponds to the two sharp peaks near zero bias in the IET spectra. Based on this model, IET spectra are fitted very well, giving the value of E_c. The details of the model can be found in our recent paper.[25]

The IET spectrum in the P state for junction C with $T_a = 375\,°C$ is shown as an example in Fig. 4(a), where the
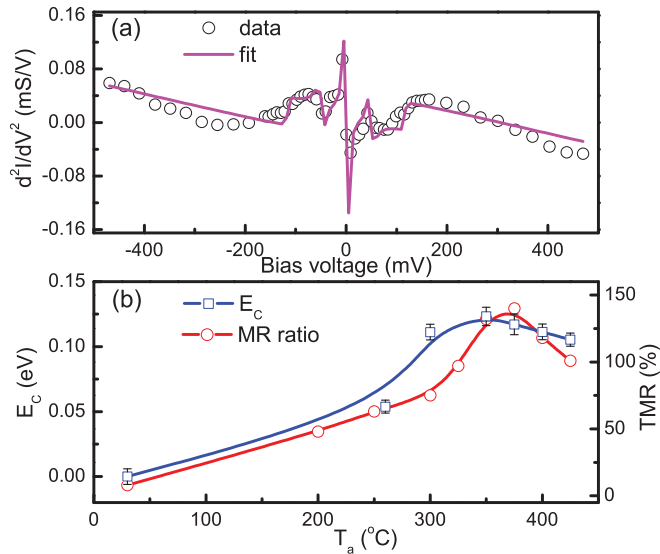
FIG. 4. (Color online) (a) IET spectra for junction C with $T_a = 375\,^\circ$C. The solid line is the fit to the data points. (b) E_c and MR ratio as a function of T_a.

FIG. 5. (Color online) XPS spectra of B 1s for samples (a) as-grown, (b) $T_a = 375\,^\circ$C, and (c) $T_a = 450\,^\circ$C, where BI, Barrier, and TI stand for the bottom interface, MgO layer, and top interface, respectively.

open circles are experimental data and the solid line is the fit based on Wei's model.[25] The fitting gives a value of activation energy E_c. Figure 4(b) shows the value of E_c and the MR ratio (for comparison) as a function of annealing temperature T_a. The value of E_c increases with increasing T_a first, then decreases with further increasing T_a, leading to a peak. To our great interest, the value of E_c and the MR ratio shows a very similar behavior. The higher the E_c, the higher is the MR ratio, and with a peak as well. This similar behavior provides clear evidence that the inelastic magnon excitation plays a major role in the annealing-temperature-dependent transport properties, especially when the MR ratio starts to decrease as $T_a > 375\,^\circ$C. The values of the MR ratio measured at 5 K were also collected (not shown here). For example, the values measured at RT for junctions annealed at 300, 375, and 400 $^\circ$C are 75%, 140%, and 118%, and the values measured at 5 K are 100%, 210%, and 160%, respectively. The MR ratio measured at 5 K shows a very similar behavior with the values measured at RT as a function of T_a. What is the origin of the similar behavior of the MR ratio and magnon activation energy E_c shown above?

During thermal annealing, the diffusion and/or motion of B atoms (from CoFeB electrodes), together with Mn diffusion (from the antiferromagnetic IrMn layer), are considered to be critical processes. In general, the formation of boron oxide or a MgBO layer from incorporating B atoms into the MgO barrier is important for the MR ratio and its bias voltage dependence.[14,30–33] The evidence of boron oxide or a MgBO layer was provided by a peak at 192.5 eV in the XPS spectra,[14,30] where the boron peak is at 188 eV. This finding was also supported by the TEM images.[30] However, based on a detailed analysis of TEM images obtained from annealed samples, the B atoms rejected from crystallized CoFeB layers were found to be dissolved in the upper amorphous Ta layer and segregated in the bottom crystalline Ta layer.[33] Obviously, the formation of boron oxide or MgBO layer during annealing should be clarified.
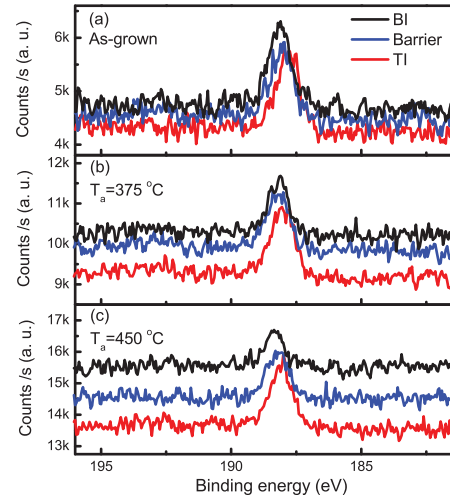
Here, the behavior of B atoms in the CoFeB layers during thermal annealing is investigated by XPS measurements carried out on a Thermo Scientific ESCALAB 250 machine. The machine is equipped with an ion milling system, enabling to "peel" away the layers step by step with a well-controlled etching rate. The XPS spectra of B 1s are shown in Fig. 5 for the three typical samples (a) as-grown sample, (b) $T_a = 375\,^\circ$C, and (c) $T_a = 450\,^\circ$C. For each sample, three typical XPS spectra collected at the top MgO/CoFeB interface (TI), in the MgO barrier, and at the bottom CoFeB/MgO interface (BI) are shown. In Fig. 5, only the B 1s peak located close to 188 eV is clearly observed. No peaks from boron oxide which located at ∼192.5 eV are observed under the current sensitivity of the Thermo Scientific ESCALAB 250 machine. Based on the above XPS results, it is reasonable to conclude that no clear peaks of boron oxide for all samples investigated here were observed. The B atoms could be dissolved in the upper amorphous Ta layer and segregated in the bottom crystalline Ta layer.[33]

Mn diffusion during annealing is very important for sputtered CoFeB/MgO/CoFeB junctions where one of the CoFeB layers is directly pinned by an antiferromagnetic IrMn layer. When T_a is higher than T_p, the MR ratio decreases with further increasing T_a, which is attributed to Mn diffusion.[10,12] Generally, Mn diffusion will have three possible effects on CoFeB/MgO/CoFeB junctions. First, the pinning effect due to exchange bias between IrMn and CoFeB layers will greatly deteriorate, and the antiparallel configuration between the bottom and top FM electrodes shows a departure from its ideal alignment (180°). This departure increases the AP conductance, leading to a lower MR ratio.[5,26] Second, Mn diffusion can cause the deterioration of the crystal structure of the CoFeB layers, which plays a negative role in spin-dependent tunneling across the MgO barrier. Third, the diffused Mn atoms are located at CoFeB/MgO interfaces or inside the MgO barrier as magnetic impurities, together with a change of the interfacial structure, which enhances the spin flipping scattering, leading to a lower MR ratio. In our case, a clear

plateau on the R-H curve for the AP state shown in the inset of Fig. 1 is seen for the annealed junctions (including $T_a = 425\,^\circ\text{C}$), which removes the departure from the ideal AP state as the origin. Furthermore, the peak position due to spin-dependent elastic tunneling (shown in Fig. 2) does not change with thermal annealing, indicating that Mn diffusion plays a negligible effect on the spin-dependent tunneling. Therefore, the diffusion of B and Mn atoms can be excluded as the origin of the MR behavior and the value of E_c for the samples investigated here. When T_a is increased beyond $500\,^\circ\text{C}$, the MR ratio decreases dramatically due to the deterioration of the exchange bias caused by the Mn diffusion.[10,12]

In summary, thermal annealing is a critical process for improving the performance of sputtered CoFeB/MgO/CoFeB junctions, however, its effect on magnetotransport properties is highly complicated. Besides the improved crystallinity of the MgO barrier and CoFeB layers and sharper interfaces between the CoFeB and MgO layers, thermal annealing plays an important role in magnon excitations. A similar behavior of the values of E_c and the MR ratio provides evidence for the contri-bution of magnon excitation to the magnetoresistance behavior. We conclude that the magnon excitation, together with improved crystallinity of the MgO barrier and CoFeB layers, contribute to the annealing-temperature-dependent MR behavior.

*Sgwang@aphy.iphy.ac.cn

[1] W. H. Butler, X.-G. Zhang, T. C. Schulthess, and J. M. MacLaren, Phys. Rev. B **63**, 054416 (2001).

[2] S. S. P. Parkin, C. Kaiser, A. Panchula, P. M. Rice, B. Hughes, M. Samant, and S. H. Yang, Nat. Mater. **3**, 862 (2004).

[3] S. Yuasa, T. Nagahama, A. Fukushima, Y. Suzuki, and K. Ando, Nat. Mater. **3**, 868 (2004).

[4] C. Tiusan, J. Faure-Vincent, C. Bellouard, M. Hehn, E. Jouguelet, and A. Schuhl, Phys. Rev. Lett. **93**, 106602 (2004).

[5] S. G. Wang, R. C. C. Ward, G. X. Du, X. F. Han, C. Wang, and A. Kohn, Phys. Rev. B **78**, 180411(R) (2008).

[6] S. Ikeda, J. Hayakawa, Y. Ashizawa, Y. M. Lee, K. Miura, H. Hasegawa, M. Tsunoda, F. Matsukura, and H. Ohno, Appl. Phys. Lett. **93**, 082508 (2008).

[7] S. Mao *et al.*, IEEE Trans. Magn. **42**, 97 (2006).

[8] C. Chappert, A. Fert, and F. Nguyen Van Dau, Nat. Mater. **6**, 813 (2007).

[9] S. Yuasa and D. D. Djayaprawira, J. Phys. D **40**, R337 (2007).

[10] C. Park, J. G. Zhu, M. T. Moneck, Y. G. Peng, and D. E. Laughlin, J. Appl. Phys. **99**, 08A901 (2006).

[11] J. Hayakawa, S. Ikeda, Y. M. Lee, F. Matsukura, and H. Ohno, Appl. Phys. Lett. **89**, 232510 (2006).

[12] S. Ikeda, J. Hayakawa, Y. M. Lee, T. Tanikawa, F. Matsukura, and H. Ohno, J. Appl. Phys. **99**, 08A907 (2006).

[13] Q. L. Ma, J. F. Feng, Gen Feng, K. Oguz, X. F. Han, and J. M. D. Coey, J. Magn. Magn. Mater. **322**, 108 (2010).

[14] J. C. Read, P. G. Mather, and R. A. Buhrman, Appl. Phys. Lett. **90**, 132503 (2007).

[15] S. G. Wang, G. Han, G. H. Yu, Y. Jiang, C. Wang, A. Kohn, and R. C. C. Ward, J. Magn. Magn. Mater. **310**, 1935 (2007).

[16] R. Matsumoto *et al.*, Solid State Commun. **143**, 574 (2007); **136**, 611 (2005).

[17] Y. Ando, J. Murai, H. Kubota, and T. Miyazaki, J. Appl. Phys. **87**, 5209 (2000).

[18] G. X. Miao, K. B. Chetry, A. Gupta, W. H. Butler, K. Tsunekawa, D. D. Djayaprawira, and G. Xiao, J. Appl. Phys. **99**, 08T305 (2006).

[19] M. Mizuguchi, Y. Hamada, R. Matsumoto, S. Nishioka, H. Maehara, K. Tsunekawa, D. D. Djayaprawira, N. Watanabe, T. Nagahama, A. Fukushima, H. Kubota, S. Yuasa, M. Shiraishi, and Y. Suzuki, J. Appl. Phys. **99**, 08T309 (2006).

[20] S. Nishioka, R. Matsumoto, H. Tomita, T. Nozaki, Y. Suzuki, H. Itoh, and S. Yuasa, Appl. Phys. Lett. **93**, 122511 (2008).

[21] K. Ono, T. Daibou, S.-J. Ahn, Y. Sakuraba, Y. Miyakoshi, M. Oogane, Y. Ando, and T. Miyazaki, J. Appl. Phys. **99**, 08A905 (2006).

[22] D. Bang, T. Nozaki, D. D. Djayaprawira, M. Shiraishi, Y. Suzuki, A. Fukushima, H. Kubota, T. Nagahama, S. Yuasa, H. Maehara, K. Tsunekawa, Y. Nagamine, N. Watanabe, and H. Itoh, J. Appl. Phys. **105**, 07C924 (2009).

[23] V. Drewello, M. Schäfers, O. Schebaum, A. A. Khan, J. Münchenberger, J. Schmalhorst, G. Reiss, and A. Thomas, Phys. Rev. B **79**, 174417 (2009).

[24] G. X. Du, S. G. Wang, Q. L. Ma, Y. Wang, R. C. C. Ward, X.-G. Zhang, C. Wang, A. Kohn, and X. F. Han, Phys. Rev. B **81**, 064438 (2010).

[25] H. X. Wei, Q. H. Qin, Q. L. Ma, X.-G. Zhang, and X. F. Han, Phys. Rev. B **82**, 134436 (2010).

[26] Q. L. Ma, S. G. Wang, J. Zhang, Y. Wang, R. C. C. Ward, C. Wang, A. Kohn, X.-G. Zhang, and X. F. Han, Appl. Phys. Lett. **95**, 052506 (2009).

[27] S. G. Wang, R. C. C. Ward, T. Hesjedal, X.-G. Zhang, C. Wang, A. Kohn, Q. L. Ma, Jia Zhang, H. F. Liu, and X. F. Han, J. Nanosci. Nanotechnol. (in press).

[28] S. Zhang, P. M. Levy, A. C. Marley, and S. S. P. Parkin, Phys. Rev. Lett. **79**, 3744 (1997).

[29] E. L. Wolf, *Principle of Electron Tunneling Spectroscopy* (Oxford University Press, New York, 1985).

[30] Y. Jang, K. Lee, S. Lee, S. Yoon, B. K. Cho, Y. J. Cho, K. W. Kim, and K. S. Kim, J. Appl. Phys. **105**, 07C901 (2009).

[31] J. Schmalhorst, A. Thomas, G. Reiss, X. Kou, and E. Arenholz, J. Appl. Phys. **102**, 053907 (2007).

[32] Y. Lu, M. Tran, H. Jaffrès, P. Seneor, C. Deranlot, F. Petroff, J. M. George, B. Lépine, S. Ababou, and G. Jézéquel, Phys. Rev. Lett. **102**, 176801 (2009).

[33] S. V. Karthik, Y. K. Takahashi, T. Ohkubo, K. Hono, S. Ikeda, and H. Ohno, J. Appl. Phys. **106**, 023920 (2009).